Published in final edited form as:
*J Neurosurg*. 2014 January ; 120(1): 152–163. doi:10.3171/2013.9.JNS13839.

# Lesion analysis for cingulotomy and limbic leucotomy: comparison and correlation with clinical outcomes

**Jimmy C. Yang, B.A.**[1,5], **Daniel T. Ginat, M.D., M.S.**[2], **Darin D. Dougherty, M.D., M.SC.**[3,5], **Nikos Makris, M.D., Ph.D.**[#4,5,6], and **Emad N. Eskandar, M.D.**[#1,5]

[1]Department of Neurosurgery, Center for Morphometric Analysis, Athinoula A. Martinos Center for Biomedical Imaging, Massachusetts General Hospital, Boston, Massachusetts

[2]Department of Imaging, Center for Morphometric Analysis, Athinoula A. Martinos Center for Biomedical Imaging, Massachusetts General Hospital, Boston, Massachusetts

[3]Department of Psychiatry, Center for Morphometric Analysis, Athinoula A. Martinos Center for Biomedical Imaging, Massachusetts General Hospital, Boston, Massachusetts

[4]Department of Neurology and Psychiatry, Center for Morphometric Analysis, Athinoula A. Martinos Center for Biomedical Imaging, Massachusetts General Hospital, Boston, Massachusetts

[5]Harvard Medical School, Psychiatry Neuroimaging Laboratory, Brigham and Women's Hospital, Boston, Massachusetts

[6]Department of Psychiatry, Psychiatry Neuroimaging Laboratory, Brigham and Women's Hospital, Boston, Massachusetts

[#] These authors contributed equally to this work.

## Abstract

**Object—**Cingulotomy and limbic leucotomy are lesioning surgeries with demonstrated benefit for medically intractable psychiatric illnesses. They represent significant refinements of the prefrontal lobotomy used from the 1930s through the 1950s. However, the associations between anatomical characterization of these lesions and outcome data are not well understood. To elucidate these procedures and associations, the authors sought to define and compare the neuroanatomy of cingulotomy and limbic leucotomy and to test a method that uses neuroanatomical data and voxel-based lesion–symptom mapping (VLSM) to reveal potential refinements to modern psychiatric neurosurgical procedures.



*Address correspondence to:* Emad N. Eskandar, M.D., Department of Neurosurgery, Massachusetts General Hospital, 55 Fruit St., White 502, Boston, MA 02114. eeskandar@partners.org..

**Disclosure** The authors report no conflict of interest concerning the materials or methods used in this study or the findings specified in this paper.

Author contributions to the study and manuscript preparation include the following. Conception and design: all authors. Acquisition of data: Yang. Analysis and interpretation of data: Eskandar, Yang, Dougherty, Makris. Drafting the article: Yang. Critically revising the article: all authors. Reviewed submitted version of manuscript: all authors. Approved the final version of the manuscript on behalf of all authors: Eskandar. Statistical analysis: Yang. Study supervision: Eskandar, Dougherty, Makris.

**Methods—**T1-weighted MR images of patients who had undergone cingulotomy and limbic leucotomy were segmented and registered onto the Montreal Neurological Institute T1-weighted template brain MNI152. Using an atlas-based approach, the authors calculated, by case, the percentage of each anatomical structure affected by the lesion. Because of the infrequency of modern lesion procedures and the requirement for higher-resolution clinical imaging, the sample size was small.

The pilot study correlated cingulotomy and limbic leucotomy lesion characteristics with clinical outcomes for patients with obsessive-compulsive disorder. For this study, preoperative and postoperative Yale-Brown Obsessive Compulsive Scale scores for 11 cingulotomy patients and 8 limbic leucotomy patients were obtained, and lesion masks were defined and compared anatomically by using an atlas-based method. Statistically significant voxels were additionally calculated by using VLSM techniques that correlated lesion characteristics with postoperative scores.

**Results—**Mean lesion volumes were 13.3 ml for cingulotomy and 11.8 ml for limbic leucotomy. As expected, cingulotomy was isolated to the anterior cingulum. The subcaudate tractotomy portion of limbic leucotomy additionally affected Brodmann area 25, the medial orbitofrontal cortex, and the nucleus accumbens.

Initial results indicated that the dorsolateral regions of the cingulotomy lesion and the posteroventral regions of the subcaudate tractotomy lesion were associated with improved postoperative Yale-Brown Obsessive Compulsive Scale scores.

**Conclusions—**Cingulotomy and limbic leucotomy are lesioning surgeries that target pathological circuits implicated in psychiatric disease. Lesion analysis and VLSM contextualize outcome data and have the potential to be useful for improving lesioning neurosurgical procedures.

## Keywords

cingulotomy; subcaudate tractotomy; limbic leucotomy; psychosurgery; lobotomy; lesion analysis; functional neurosurgery

---

The field of psychiatric neurosurgery was spurred in 1935 by the work of neurologist Egas Moniz and neurosurgeon Almeida Lima in prefrontal lobotomy, which sought to sever connections in the frontal lobes that were thought to cause psychiatric symptoms.[32,53,57,73] In 1947, Spiegel developed the stereotactic frame, which enabled the creation of lesions at specific targets for psychosurgery,[81] providing the original basis for the modern cingulotomy, subcaudate tractotomy, and limbic leucotomy. With these advances in surgical technology and the development of medical therapies for psychiatric illness, lobotomy largely disappeared around the 1950s.[53,73,88]

For patients with obsessive-compulsive disorder (OCD) that is refractory to optimal medical management, lesioning procedures offer reduction or complete relief of symptoms.[15,24,26,35,53,58] Cingulotomy involves stereotactically creating lesions in the anterior cingulate gyrus to interrupt the cingulum bundle.[6,7,20,31,47,49] In the context of OCD, outcomes for patients who have undergone cingulotomy have been positive; rates of

adverse effects have been low, and symptoms have improved for 30%–50% of patients.[24,26,37] With slightly higher symptom improvement rates (approximately 65%[15,35]) among OCD patients, subcaudate tractotomy creates lesions in the white matter below the head of the caudate nucleus, targeting corticostriatothalamic pathways.[26,42,53] The combination of these 2 stereotactic surgeries is the limbic leucotomy,[39,53] and the limited outcome data available show improvement for approximately 36%[58]–62%[34] of OCD patients. Studies examining a 2-stage limbic leucotomy at our institution (Massachusetts General Hospital), in which subcaudate tractotomy is performed if symptoms remain refractory to treatment after anterior cingulotomy, have shown that symptoms improve for 73% of OCD patients.[13]

Based on advances in MRI, modern lesion analysis offers a method for understanding how lesion morphometry, volume, and location are associated with changes in function, indicated by changes in behavior. Although these lesion analysis studies have been chiefly conducted in the area of stroke,[16,17,51] similar methods have been applied to psychiatric neurosurgery.[71,72] Recent advances in lesion analysis have moved the field toward a voxel-based approach. Voxel-based lesion–symptom mapping (VLSM) correlates coregistered lesion characteristics with behavioral output.[8] This modality is advantageous because it examines continuous behavioral variables and entire lesion masks instead of substitutes like center-of-mass coordinates. Statistics are subsequently calculated on the basis of behavioral scores for each voxel. As a result, patients do not need to be initially classified by either lesion location or behavioral scores.[8] This method has been primarily applied to patients with stroke or traumatic brain injury to better understand the anatomical areas that are crucial for gesture recognition,[38] reversal learning,[87] language,[5,30] gait asymmetry,[4] and facial emotion recognition.[21]

Although modern psychiatric neurosurgical procedures have been shown to be effective, it is not clear why only certain patients respond. As a result, we used MR-based imaging tools for lesion analysis to define the neuroanatomy of anterior cingulotomy and limbic leucotomy. In addition, we used resulting lesion morphometry and volumetry to compare lesions to find differences among the procedures. Finally, we performed a pilot study in which we applied these tools with VLSM to demonstrate how these approaches can be used to refine psychiatric neurosurgical procedures.

## Methods

### Patient Characteristics

The Massachusetts General Hospital Institutional Review Board approved this retrospective study. Patients who had undergone dorsal anterior cingulotomy and limbic leucotomy, with clinical T1-weighted MRI (slice thickness ≤ 3.4 mm), were identified from a Massachusetts General Hospital database of patients maintained since 1992. Procedures were performed by 2 neurosurgeons who used the same technique, as verified by operative reports. It should be noted that anterior cingulotomy and limbic leucotomy procedures are uncommon, but the case volume at Massachusetts General Hospital is one of the largest world-wide. Although studies that examine only the outcomes of modern psychosurgical lesioning procedures have

larger sample sizes than the study presented here, lesion analysis of these procedures is uncommon; studies have incorporated follow-up data for 8 patients[82] and 15 patients.[74]

**Dorsal Anterior Cingulotomy—**We identified 18 patients (10 male, 8 female) who had undergone dorsal anterior cingulotomy during 1999–2011. Mean age (± standard error) at the time of surgery was 36.9 ± 2.9 years. The most common indication for cingulotomy (13 patients) was OCD.

Cingulotomy surgery involved stereotactic placement of 6 total lesions (3 per side) in the anterior cingulate gyrus (Fig. 1). Lesions were made by thermocoagulation with an electrode with a 10-mm exposed tip (Cosman Medical). Coordinates were tailored for each patient and guided by neurophysiological recordings to verify placement in the cingulate gyrus; patients were continuously monitored for adverse effects during surgery. In general, lesions were placed 20 mm posterior to the anterior extent of the frontal horn of the lateral ventricles, 5–7 mm off the midline, and 5 mm above the corpus callosum. Subsequent lesions were placed 6–7 mm anteriorly and 1–2.5 mm inferiorly.

**Limbic Leucotomy—**We identified 11 patients (5 male, 6 female) who had undergone limbic leucotomy from 2001 to 2008. Mean age (± standard error) at the time of surgery was 39.3 ± 3.6 years. The most common indication for limbic leucotomy (8 patients) was OCD.

Lesions were again made by heating an electrode with a 10-mm exposed tip. Limbic leucotomy was completed with the addition of a subcaudate tractotomy lesion after anterior cingulotomy. Subcaudate tractotomy involved 4 total lesions (2 per side) (Fig. 1). Coordinates were again tailored for each patient and guided by neurophysiological recordings to verify placement, and patients were continuously monitored for adverse effects during surgery. In general, the medial lesions were placed 7 mm lateral to the midline, 5–7 mm off the floor, and 7 mm anterior to the sylvian fissure. The lateral lesion was made 7–8 mm lateral to the first.

**Follow-Up Data—**Retrospective follow-up data were obtained for 15 patients whose indication for anterior cingulotomy and/or limbic leucotomy was OCD that was refractory to medical management. These patients met criteria for OCD as outlined in the Diagnostic and Statistical Manual of Mental Disorders editions III, III-R, or IV, and the OCD was nonresponsive to conventional treatment, defined as at least 3 selective serotonin reuptake inhibitors, 2 augmentation agents, and behavioral therapy. Preoperative and postoperative Yale-Brown Obsessive Compulsive Scale (Y-BOCS) scores were obtained, and long-term follow-up information was obtained by review of electronic medical records and phone interviews. For 11 patients (8 male, 3 female), anterior cingulotomy lesions were correlated with outcome; mean age (± standard error) at time of surgery was 33.0 ± 2.7 years. For 8 patients (5 male, 3 female), limbic leucotomy lesions were also correlated with outcome; mean age (± standard error) at the time of surgery was 34.7 ± 2.5 years.

## Acquisition of MR Images

Magnetic resonance images were obtained as part of standard clinical care. Anterior cingulotomy and limbic leucotomy images were obtained within 5 postoperative days. T1-

weighted images were used for lesion segmentation and analysis. Representative parameters on a GE 1.5 T Signa (GE Healthcare) scanner were as follows: TR/TE = 8.3/3.4 msec, flip angle 30°, matrix 256 × 192, pixel bandwidth 122.1 Hz, and display FOV 220 mm. Because lesions created during cingulotomy and limbic leucotomy are small, inclusion criteria included maximum slice thickness of 3.4 mm and maximum spacing of 1.7 mm.

### Morphometric Lesion Analysis

Images were analyzed at the Massachusetts General Hospital Center for Morphometric Analysis at the Athinoula A. Martinos Center for Biomedical Imaging. T1-weighted images were segmented in Freeview, part of the FreeSurfer imaging software package developed by the Athinoula A. Martinos Center. The resulting output was a mask of the lesion (Fig. 2).

Because clinical MR images were not consistently of the complete brain, because they were of lower resolution (compared with images used specifically for research), and because of the presence of lesions that could cause automated registration to fail,[41] we implemented a linear, manual, landmark-based registration that used 12 degrees of freedom. The landmarks were the anterior commissure, the posterior commissure, and the interhemispheric plane.[27,86] This method involves alignment of the centroids of 2 landmarks, followed by rotation and scaling of the image to minimize displacements. Imaging data from each patient were registered onto the Montreal Neurological Institute (MNI) brain MNI152, which is the average of 152 T1-weighted MR images in MNI space. Figure 3 displays the distribution of postregistration lesions for cingulotomy and limbic leucotomy patients, presented as a heat map. Segmentation and registration were performed by 1 author (J.C.Y.) and subsequently corroborated by a neuroanatomist (N.M.); both were blinded as to postoperative outcomes. Intrarater reliability was determined by re-segmenting the lesions in a random selection of patients and calculating the percentage of overlapping voxels. This method consequently serves as a metric for volumetric and spatial reliability. In addition, intrarater reliability was further quantified by calculation of the Cronbach alpha in SPSS.

Anatomical overlap data were calculated by using 2 built-in atlases in the FMRIB Software Library (The Oxford Centre for Functional MRI of the Brain, University of Oxford, Oxford, UK): the Jülich histological atlas and the Johns Hopkins University white-matter tractography atlas; the third atlas used was the Center for Morphometric Analysis structural atlas[18,52,56,67,69] (Fig. 4). The Jülich histological atlas is based on microscopic and histological examination of 10 postmortem brains, and the Johns Hopkins University white-matter tractography atlas uses the probabilistic average of deterministic tractography results on 28 healthy participants. Probability level was set at a threshold of 0.05, indicating the white matter tracts of 95% of participants. The result of this analysis was the number of voxels that overlapped between the anatomical region of interest (ROI) and the lesion.

The degree to which an atlas-based ROI was affected by the lesion was calculated as a percentage overlap, defined as the number of voxels in the lesion found to overlap with the ROI, divided by the total number of voxels for that ROI. Lesion volumes were calculated by multiplying the number of voxels in each coronal image by the volume per voxel. Given the small sample size and nonnormal distribution, we performed a 2-tailed Wilcoxon rank-sum test to determine statistical significance. Error is reported as standard error.

Voxel-based lesion–symptom mapping was done by using MRIcron and nonparametric mapping software[75] (McCausland Center for Brain Imaging, University of South Carolina). Statistics were calculated with a false-detection rate of 5% with the nonparametric Brunner-Munzel test because of nonparametric outcome scores. Given the small sample size but generally extensive overlap among lesions, voxels with ≥ 2 patients were included in the analysis.

Lesions and ROIs were visualized by using Freeview, FSLView (part of the FMRIB Software Library), and MRIcron.

## Results

### Lesion Volume

Lesion volume was calculated from lesion segmentation (Fig. 5). Mean (± standard error) cingulotomy lesion volume was 13.3 ± 0.7 ml, which was similar to the mean limbic leucotomy volume of 11.8 ± 0.9 ml. Intrarater reliability calculations were based on percentage of overlapping voxels in a random selection of patients who underwent lesion segmentation twice; reliability was 91%. With respect to lesion volume, the Cronbach alpha was high (0.98).

### Lesion Anatomical Overlap

A total of 683 ROIs were investigated by using this atlas-based approach (Table 1, Figs. 6 and 7).

**Anterior Cingulotomy—**The predominant structures in which lesions were created by anterior cingulotomy were the bilateral anterior cingula and cingulate gyri (corresponding with Brodmann areas 24 and 32) (Table 1, Figs. 6 and 7). On the basis of the Johns Hopkins University white-matter and the Center for Morphometric Analysis atlases, the difference in overlap between the left and right cingula and cingulate gyri was not significant.

**Limbic Leucotomy—**Approximately 80% of the area of the nucleus accumbens was affected by limbic leucotomy, and although the cingula and cingulate gyri were affected by the matured cingulotomy lesion, the paraterminal gyrus (Brodmann area 25) and subgenual cingulate were lesioned by the subcaudate tractotomy (Table 1, Fig. 7). Notable white matter structures that overlapped with the limbic leucotomy lesion included the bilateral uncinate fascicles and the white matter of the medial orbitofrontal cortex (Table 1, Fig. 6). Comparison of the bilateral lesions demonstrated no significant difference in anatomical overlap on the right versus the left sides.

### Lesion Characteristics and Clinical Outcomes

Our pilot study elucidated the relationship between lesion characteristics and clinical outcomes in a subgroup of patients for whom lesioning surgery was indicated for medically intractable OCD. Unfortunately, sample size was limited because of the infrequency with which these procedures were performed and the requirement for higher resolution postoperative clinical imaging. We analyzed data from 11 anterior cingulotomy patients and

8 limbic leucotomy patients. The data were analyzed in 2 ways. The first method, a categorical comparison, divided the patients into responders and nonresponders according to Y-BOCS scores at a threshold of ≥ 35% decrease in Y-BOCS postoperative score[62] (Table 2, Fig. 8) and subsequently analyzed and compared anatomical overlap data for each ROI (Tables 3 and 4). The second method involved VLSM with postoperative Y-BOCS scores.

**Categorical Comparison—**Among the 11 patients who underwent anterior cingulotomy, 9 were considered nonresponders; mean (± standard error) follow-up time was 35.4 ± 13.2 months, and average Y-BOCS score decrease was 4.5% ± 3.3%. The other 2 patients were classified as responders; Y-BOCS decreases were 35% or greater, and the average Y-BOCS decrease was 66%. Lesion volumes did not differ significantly between the 2 groups. Analysis of anatomical ROI overlap of the 2 outcome groups did not find statistically significant differences in involvement of the cingulate gyrus or cingulum (Table 3).

Among the 8 patients who underwent limbic leucotomy, 4 were considered nonresponders; mean (± standard error) follow-up time was 49.0 ± 17.6 months, and average Y-BOCS decrease was 13.5 ± 6.8%. The other 4 patients were classified as responders; mean follow-up time was 25.7 ± 14.5 months. Y-BOCS decreases were ≥ 35%, and the average Y-BOCS decrease was 61.8 ± 12.9%. Lesion volumes did not differ significantly between the 2 groups. Only 1 structure, the right sublenticular extended amygdala, showed a statistically significant difference in overlap between responders and nonresponders (Table 4).

**Voxel-Based Lesion–Symptom Mapping—**A second method for analyzing the lesion and clinical data involved VLSM with postoperative Y-BOCS scores. As a result, this method does not require the grouping of patients into responders and nonresponders; instead, it compares continuous outcomes on a voxel-wise basis by using coregistered lesion masks. Because of the small sample size, a limited number of voxels was significantly correlated with improved outcomes for patients with anterior cingulotomy and limbic leucotomy lesions (Fig. 8). Dorsolateral voxels in postoperative and mature anterior cingulotomy lesions were correlated with lower postoperative Y-BOCS scores. Furthermore, for the subcaudate tractotomy portion of the limbic leucotomy, posteroventral voxels were correlated with lower postoperative Y-BOCS scores.

## Discussion

We used MRI-based and atlas-based approaches to lesion analysis to achieve a neuroanatomical understanding of cingulotomy and limbic leucotomy. Using these data, we were able to compare the areas affected by these lesions. Ultimately, anterior cingulotomy and limbic leucotomy isolated lesions to the specific aberrant circuits involved in psychopathology. This study offers a neuroanatomical characterization of anterior cingulotomy and limbic leucotomy performed at our institution and elucidates the lesion sites that result in symptom reduction.

Studies have shown that the predominant anatomical structures implicated in OCD psychopathology include the orbitofrontal cortex, anterior cingulate cortex, dorsolateral prefrontal cortex, and ventromedial prefrontal cortex.[12] Because of its role in regulation of

emotions, motivation, and behavioral planning, which has been linked to compulsions, obsessions, and intrusive thoughts, the orbitofrontal cortex influences the presentation of psychiatric symptoms.[12,23] Similarly important, the anterior cingulate cortex probably triggers repetitive behaviors through its involvement in conflict monitoring.[11,12,22,40] The ventromedial prefrontal cortex and the dorsolateral prefrontal cortex have also been associated with psychiatric symptoms. The ventromedial prefrontal cortex modulates emotional state and is involved in production of negative emotion and self-reflection.[44,68,90] Although the dorsolateral prefrontal cortex is typically characterized by its executive or cognitive functions, it also regulates and suppresses negative emotion.[33,44,48,65]

These structures are linked via the corticostriatothalamocortical circuit, which has been implicated in OCD and includes the amygdala, mediodorsal thalamus, and ventral striatum.[12,33] Meta-analyses have shown that patients with OCD have reduced gray matter density in the dorsolateral prefrontal cortex and orbitofrontal cortex and reduced volume of the anterior cingulate cortex and orbitofrontal cortex.[77,78,85] In addition, functional MRI and positron emission tomography studies of OCD patients have shown that stimulus presentation activates the orbitofrontal cortex, dorsolateral prefrontal cortex, anterior cingulate cortex, and basal ganglia structures.[2,14,23,55,70,76] In line with these findings, successful treatment of OCD by pharmacological, behavioral, and neurosurgical methods reduces activity in this circuit.[9,33,63,80,84]

Our data show that anterior cingulotomy, subcaudate tractotomy, and limbic leucotomy affect OCD circuits by directly involving the anatomical centers and connecting white matter. For example, in limbic leucotomy lesions, involvement of the bilateral uncinate fasciculi suggests severing of the connection among cortical areas and ventral prefrontal cortex and orbitofrontal cortex, which has been previously demonstrated in nonhuman primates.[46,64] As expected, given that the limbic leucotomy is a combination of anterior cingulotomy and subcaudate tractotomy, structures affected by anterior cingulotomy were included in limbic leucotomy. Involvement of the bilateral accumbens areas, ventromedial prefrontal cortex, medial and lateral orbitofrontal cortex, and Brodmann area 25, which is commonly implicated in mood,[36] were essentially unique to the limbic leucotomy.

Lesion volumetry for anterior cingulotomy shows that volumes are larger than those previously reported from our institution, likely resulting from change in procedure from creation of a single lesion in each dorsal anterior cingulum to creation of 3 lesions per side.[71] In addition, we found that, although the limbic leucotomy procedure involves both an anterior cingulotomy and subcaudate tractotomy, the mean volume of the limbic leucotomy lesion was smaller than that of the anterior cingulotomy. Although the difference in volume was not significant according to the Wilcoxon rank-sum test, this difference most likely results from the number of total lesions made (4 for subcaudate tractotomy vs 6 for anterior cingulotomy) and to contraction of the anterior cingulotomy lesion with maturity (Figs. 1–3).

For historical interest, we compared data from modern lesioning techniques with those from an MRI data set of 3 lobotomy cases (Fig. 9). Given that decades had passed between the lobotomy procedure and the time of imaging, this data set is necessarily limited by

Wallerian and age-related degeneration. However, because of the impossibility of contemporaneous MRI imaging, this data set provides the best possible description of lobotomy anatomy. Lesion size for this data set was found to be much larger than that of modern lesioning techniques; mean (± standard error) volume was 84.6 ± 1.9 ml. Similar to findings of prior studies,[10,59,61,83] numerous white and gray matter structures were involved in these lesions, including the superior sagittal stratum, anterior thalamic radiations, inferior frontal gyrus, Brodmann areas 44 and 45, cingula, medial orbitofrontal cortex, and dorsolateral prefrontal cortex. Lesioning of these structures probably explains the known side effects of lobotomy, such as emotional flattening, postoperative seizures, and changes to cognitive function and personality.[25,28,29,43,54,88] In fact, the original development of stereotactic psychiatric lesioning procedures in part aimed to avoid thalamofrontal connections to minimize the adverse effect of emotional flattening.[43]

Lesion analysis for psychiatric neurosurgical lesioning procedures is ultimately important for not only better understanding the sites affected but also for clarifying potential variation among patients and procedures performed at psychiatric neurosurgery centers. Given that these procedures often vary according to institution, lesion analysis is an avenue for contextualizing reported outcomes, based on the structures affected. Moreover, as shown by our pilot study of a method that reveals the most important parts of lesions for symptomatic improvement, lesion analysis can be used to refine psychiatric neurosurgery techniques.

In the context of treatment of medically intractable OCD, the most recently reported success rates are in the range of 30%–50% for cingulotomy[24,26,37] and 36%–50% for limbic leucotomy.[58] However, we do not have an optimal understanding of why only a proportion of surgeries are successful. Modern techniques in lesion analysis might enable us to correlate clinical outcome with lesion characteristics. Ultimately, adoption of these techniques might lead to an understanding of lesion–outcome relationships.

Although extensive lesion analysis has not been reported for limbic leucotomy, 2 studies have explicitly applied lesion analysis to cingulotomy lesions to better understand if lesion characteristics are related to postoperative patient outcomes.[74,82] Richter et al. found that more dorsal lesions resulted in superior clinical response in terms of Y-BOCS score improvement, but whether this finding was statistically significant is unclear because only 1 patient had lasting benefit for more than 1 year.[74] In the context of depression, Steele et al. found that smaller and more anterior lesions garnered better clinical response at 1 year in 8 patients,[82] although this study focused on center-of-mass lesion locations rather than lesions as a whole.

We did not find that anterior cingulotomy lesion volume was associated with outcome for patients with OCD. However, our small sample size was skewed, given that only 2 of the patients examined were classified as responders. In addition, these previous studies involve a different lesion technique than the one currently used at our institution.

Comparison of responder and nonresponder anterior cingulotomy patients did not reveal statistically significant differences in anatomical areas affected. Although this result might be caused by small sample size, another reason might be the location-specific nature of

surgical outcome. Voxel-based lesion–symptom mapping demonstrates that dorsolateral and anterior aspects of the anterior cingulotomy lesion were correlated with improved outcome, a finding that is similar to that of Steele et al.[82] and Richter et al.[74] It is potentially more powerful than direct comparison of structures because it uses a voxelwise approach and continuous outcome variables, which make it unnecessary to group patients according to responder category.

In our small sample size of 8 limbic leucotomy patients, we found that lesion volume did not predict patient outcome. Voxel-based lesion–symptom mapping suggested that more posteroventral subcaudate tractotomy lesions are associated with improved outcome. Only 1 structure was associated with improved outcome: the sublenticular extended amygdala. The amygdala receives multiple sensory inputs and, given its links to the limbic areas, could link these inputs to emotions.[3] Volumetric MRI studies have also shown that OCD patients have significantly enlarged left amygdala volume.[45] Moreover, in rats, the sublenticular extended amygdala specifically has been shown to be involved in reward processes via the medial forebrain bundle.[89] In humans, the sublenticular extended amygdala is thought to have a role in emotional salience processing,[50,66] and functional MRI studies have shown activation of the sublenticular extended amygdala during expectation of negative stimuli in patients with major depression.[1] As a result, it is plausible that modulation of this region could lead to improved outcomes for OCD patients.

This study's predominant limitation is its small sample size. Nevertheless, this study demonstrates the usefulness of applying lesion analysis based on anatomical overlap and VLSM to the refinement of future psychiatric neurosurgical procedures. Development of a database of patient outcomes and lesion masks will probably lead to correlation of lesioned areas with improved clinical outcome. Using these data, surgeons can tailor procedures to target regions correlated with improved success rates. This study's other limitations include its nonstandardized imaging parameters (because of the clinical setting in which they were obtained) and relatively lower quality of imaging.

An extension of these lesion analysis techniques would incorporate recent advances in diffusion imaging to characterize the specific connectivities affected by each lesion type. Recent studies with diffusion tensor imaging have shown differences in connectivity in patients with OCD.[19,60] One diffusion study investigated the association between psychiatric neurosurgical lesions, including anterior cingulotomy, subcaudate tractotomy, and limbic leucotomy, and white matter tracts but used simulated lesions and healthy participants.[79] As a result, further research would investigate patient-specific white matter tracts and determine whether anterior cingulotomy and limbic leucotomy must interrupt specific tracts for improved outcomes.

## Conclusions

Anterior cingulotomy and limbic leucotomy arose from the prefrontal lobotomy of the 1930s–1950s, but these newer procedures affect specific pathological circuits, resulting in increased efficacy and reduced adverse effects. Both procedures target the corticostriatothalamocortical circuit implicated in OCD, particularly at anatomical centers

that are differentially activated in symptomatic patients. Modern lesion analysis with MRI-based techniques can characterize the lesions caused by these procedures morphometrically and volumetrically. This characterization is particularly useful for contextualizing surgical outcomes, given the institution-specific approaches to these procedures. According to the results of our pilot study, correlation of lesion characteristics with outcome using lesion analysis and VLSM is a viable technique for understanding why only certain patients respond favorably to surgery and may prove useful for refining these procedures in the future.

## Acknowledgments

We thank George Papadimitriou for his assistance with image processing.

Funding was provided by the National Institute on Drug Abuse (grant no. 1R01DA027804-01 to N.M.) and National Institute of Mental Health (grant no. 1R21MH084041-01A1 to N.M.).

## Abbreviations used in this paper

| | |
|---|---|
| **OCD** | obsessive-compulsive disorder |
| **MNI** | Montreal Neurological Institute |
| **ROI** | region of interest |
| **VLSM** | voxel-based lesion–symptom mapping |
| **Y-BOCS** | Yale-Brown Obsessive Compulsive Scale. |

## References

1. Abler B, Erk S, Herwig U, Walter H. Anticipation of aversive stimuli activates extended amygdala in unipolar depression. J Psychiatr Res. 2007; 41:511–522. [PubMed: 17010993]
2. Adler CM, McDonough-Ryan P, Sax KW, Holland SK, Arndt S, Strakowski SM. fMRI of neuronal activation with symptom provocation in unmedicated patients with obsessive compulsive disorder. J Psychiatr Res. 2000; 34:317–324. [PubMed: 11104844]
3. Aggleton JP. The contribution of the amygdala to normal and abnormal emotional states. Trends Neurosci. 1993; 16:328–333. [PubMed: 7691009]
4. Alexander LD, Black SE, Patterson KK, Gao F, Danells CJ, McIlroy WE. Association between gait asymmetry and brain lesion location in stroke patients. Stroke. 2009; 40:537–544. [PubMed: 19109546]
5. Baldo JV, Wilkins DP, Ogar J, Willock S, Dronkers NF. Role of the precentral gyrus of the insula in complex articulation. Cortex. 2011; 47:800–807. [PubMed: 20691968]
6. Ballantine HT Jr, Bouckoms AJ, Thomas EK, Giriunas IE. Treatment of psychiatric illness by stereotactic cingulotomy. Biol Psychiatry. 1987; 22:807–819. [PubMed: 3300791]
7. Ballantine HT Jr, Cassidy WL, Flanagan NB, Marino R Jr. Stereotaxic anterior cingulotomy for neuropsychiatric illness and intractable pain. J Neurosurg. 1967; 26:488–495. [PubMed: 5337782]
8. Bates E, Wilson SM, Saygin AP, Dick F, Sereno MI, Knight RT, et al. Voxel-based lesion-symptom mapping. Nat Neurosci. 2003; 6:448–450. [PubMed: 12704393]
9. Baxter LR Jr, Schwartz JM, Bergman KS, Szuba MP, Guze BH, Mazziotta JC, et al. Caudate glucose metabolic rate changes with both drug and behavior therapy for obsessive-compulsive disorder. Arch Gen Psychiatry. 1992; 49:681–689. [PubMed: 1514872]
10. Benson DF, Stuss DT, Naeser MA, Weir WS, Kaplan EF, Levine HL. The long-term effects of prefrontal leukotomy. Arch Neurol. 1981; 38:165–169. [PubMed: 7469849]

11. Botvinick M, Nystrom LE, Fissell K, Carter CS, Cohen JD. Conflict monitoring versus selection-for-action in anterior cingulate cortex. Nature. 1999; 402:179–181. [PubMed: 10647008]
12. Bourne SK, Eckhardt CA, Sheth SA, Eskandar EN. Mechanisms of deep brain stimulation for obsessive compulsive disorder: effects upon cells and circuits. Front Integr Neurosci. 2012; 6:29. [PubMed: 22712007]
13. Bourne SK, Sheth SA, Neal J, Strong C, Mian MK, Cosgrove GR, et al. Beneficial effect of subsequent lesion procedures after nonresponse to initial cingulotomy for severe, treatment-refractory obsessive-compulsive disorder. Neurosurgery. 2013; 72:196–202. [PubMed: 23147780]
14. Breiter HC, Rauch SL, Kwong KK, Baker JR, Weisskoff RM, Kennedy DN, et al. Functional magnetic resonance imaging of symptom provocation in obsessive-compulsive disorder. Arch Gen Psychiatry. 1996; 53:595–606. [PubMed: 8660126]
15. Bridges PK, Bartlett JR, Hale AS, Poynton AM, Malizia AL, Hodgkiss AD. Psychosurgery: stereotactic subcaudate tractomy. An indispensable treatment. Br J Psychiatry. 1994; 165:599–613. [PubMed: 7866675]
16. Caviness VS, Makris N, Montinaro E, Sahin NT, Bates JF, Schwamm L, et al. Anatomy of stroke, Part I: an MRI-based topographic and volumetric system of analysis. Stroke. 2002; 33:2549–2556. [PubMed: 12411641]
17. Caviness VS, Makris N, Montinaro E, Sahin NT, Bates JF, Schwamm L, et al. Anatomy of stroke, Part II: volumetric characteristics with implications for the local architecture of the cerebral perfusion system. Stroke. 2002; 33:2557–2564. [PubMed: 12411642]
18. Caviness VS Jr, Meyer J, Makris N, Kennedy DN. MRI-based topographic parcellation of human neocortex: an anatomically specified method with estimate of reliability. J Cogn Neurosci. 1996; 8:566–587. [PubMed: 23961985]
19. Chiu CH, Lo YC, Tang HS, Liu IC, Chiang WY, Yeh FC, et al. White matter abnormalities of fronto-striato-thalamic circuitry in obsessive-compulsive disorder: a study using diffusion spectrum imaging tractography. Psychiatry Res. 2011; 192:176–182. [PubMed: 21546223]
20. Corkin S. Hidden-figures-test performance: lasting effects of unilateral penetrating head injury and transient effects of bilateral cingulotomy. Neuropsychologia. 1979; 17:585–605. [PubMed: 522973]
21. Dal Monte O, Krueger F, Solomon JM, Schintu S, Knutson KM, Strenziok M, et al. A voxel-based lesion study on facial emotion recognition after penetrating brain injury. Soc Cogn Af fect Neurosci. 2013; 8:632–639.
22. Del Casale A, Kotzalidis GD, Rapinesi C, Serata D, Ambrosi E, Simonetti A, et al. Functional neuroimaging in obsessive-compulsive disorder. Neuropsychobiology. 2011; 64:61–85. [PubMed: 21701225]
23. den Braber A, van 't Ent D, Cath DC, Wagner J, Boomsma DI, de Geus EJ. Brain activation during cognitive planning in twins discordant or concordant for obsessive-compulsive symptoms. Brain. 2010; 133:3123–3140. [PubMed: 20823085]
24. Dougherty DD, Baer L, Cosgrove GR, Cassem EH, Price BH, Nierenberg AA, et al. Prospective long-term follow-up of 44 patients who received cingulotomy for treatment-refractory obsessive-compulsive disorder. Am J Psychiatry. 2002; 159:269–275. [PubMed: 11823270]
25. Engelborghs S, Borggreve F, Pickut BA, Michiels K, Van de Mosselaer W, De Deyn PP. Case report of a patient with complex partial frontal lobe seizures as a complication of bifrontal lobotomy. Acta Neurol Belg. 1998; 98:199–203. [PubMed: 9686281]
26. Feldman RP, Alterman RL, Goodrich JT. Contemporary psychosurgery and a look to the future. J Neurosurg. 2001; 95:944–956. [PubMed: 11765838]
27. Filipek PA, Richelme C, Kennedy DN, Caviness VS Jr. The young adult human brain: an MRI-based morphometric analysis. Cereb Cortex. 1994; 4:344–360. [PubMed: 7950308]
28. Freeman W. Leucotomy in England and Wales 1942–1954. Ministry of Health Reports on Public Health and Medical Subjects No. 104. Am J Psychiatry. 1962; 118:669. Letter.
29. Freeman W. Prefrontal lobotomy: final report of 500 Freeman and Watts patients followed for 10 to 20 years. South Med J. 1958; 51:739–745. [PubMed: 13556182]

30. Geva S, Jones PS, Crinion JT, Price CJ, Baron JC, Warburton EA. The neural correlates of inner speech defined by voxel-based lesion-symptom mapping. Brain. 2011; 134:3071–3082. [PubMed: 21975590]
31. González ER. Treating the brain by cingulotomy. JAMA. 1980; 244:2141–2143. 2146–2147. [PubMed: 6775102]
32. Gross D, Schäfer G. Egas Moniz (1874–1955) and the “invention” of modern psychosurgery: a historical and ethical reanalysis under special consideration of Portuguese original sources. Neurosurg Focus. 2011; 30(2):E8. [PubMed: 21284454]
33. Haber SN, Brucker JL. Cognitive and limbic circuits that are affected by deep brain stimulation. Front Biosci (Landmark Ed). 2009; 14:1823–1834. [PubMed: 19273166]
34. Hay P, Sachdev P, Cumming S, Smith JS, Lee T, Kitchener P, et al. Treatment of obsessive-compulsive disorder by psychosurgery. Acta Psychiatr Scand. 1993; 87:197–207. [PubMed: 8096667]
35. Hodgkiss AD, Malizia AL, Bartlett JR, Bridges PK. Outcome after the psychosurgical operation of stereotactic subcaudate tractotomy, 1979–1991. J Neuropsychiatry Clin Neurosci. 1995; 7:230–234. [PubMed: 7626968]
36. Holtzheimer PE, Mayberg HS. Stuck in a rut: rethinking depression and its treatment. Trends Neurosci. 2011; 34:1–9. [PubMed: 21067824]
37. Jung HH, Kim CH, Chang JH, Park YG, Chung SS, Chang JW. Bilateral anterior cingulotomy for refractory obsessive-compulsive disorder: long-term follow-up results. Stereotact Funct Neurosurg. 2006; 84:184–189. [PubMed: 16912517]
38. Kalénine S, Buxbaum LJ, Coslett HB. Critical brain regions for action recognition: lesion symptom mapping in left hemisphere stroke. Brain. 2010; 133:3269–3280. [PubMed: 20805101]
39. Kelly D, Richardson A, Mitchell-Heggs N. Stereotactic limbic leucotomy: neurophysiological aspects and operative technique. Br J Psychiatry. 1973; 123:133–140. [PubMed: 4582234]
40. Kerns JG, Cohen JD, MacDonald AW III, Cho RY, Stenger VA, Carter CS. Anterior cingulate conflict monitoring and adjustments in control. Science. 2004; 303:1023–1026. [PubMed: 14963333]
41. Kimberg DY, Coslett HB, Schwartz MF. Power in Voxel-based lesion-symptom mapping. J Cogn Neurosci. 2007; 19:1067–1080. [PubMed: 17583984]
42. Knight GC. Bi-frontal stereotactic tractotomy: an atraumatic operation of value in the treatment of intractable psychoneurosis. Br J Psychiatry. 1969; 115:257–266. [PubMed: 4893673]
43. Knight GG. Neurosurgical aspects of psychosurgery. Proc R Soc Med. 1972; 65:1099–1104. [PubMed: 4568539]
44. Koenigs M, Grafman J. The functional neuroanatomy of depression: distinct roles for ventromedial and dorsolateral pre-frontal cortex. Behav Brain Res. 2009; 201:239–243. [PubMed: 19428640]
45. Kwon JS, Shin YW, Kim CW, Kim YI, Youn T, Han MH, et al. Similarity and disparity of obsessive-compulsive disorder and schizophrenia in MR volumetric abnormalities of the hippo-campus-amygdala complex. J Neurol Neurosurg Psychiatry. 2003; 74:962–964. [PubMed: 12810792]
46. Lehman JF, Greenberg BD, McIntyre CC, Rasmussen SA, Haber SN. Rules ventral prefrontal cortical axons use to reach their targets: implications for diffusion tensor imaging tractography and deep brain stimulation for psychiatric illness. J Neurosci. 2011; 31:10392–10402. [PubMed: 21753016]
47. Leiphart JW, Valone FH III. Stereotactic lesions for the treatment of psychiatric disorders. A review. J Neurosurg. 2010; 113:1204–1211. [PubMed: 20560726]
48. Lévesque J, Eugène F, Joanette Y, Paquette V, Mensour B, Beaudoin G, et al. Neural circuitry underlying voluntary suppression of sadness. Biol Psychiatry. 2003; 53:502–510. [PubMed: 12644355]
49. Lewin W. Observations on selective leucotomy. J Neurol Neurosurg Psychiatry. 1961; 24:37–44. [PubMed: 13761674]
50. Liberzon I, Phan KL, Decker LR, Taylor SF. Extended amygdala and emotional salience: a PET activation study of positive and negative affect. Neuropsychopharmacology. 2003; 28:726–733. [PubMed: 12655318]

51. Makris N, Caviness VS, Kennedy DN. An introduction to MR imaging-based stroke morphometry. Neuroimaging Clin N Am. 2005; 15:325–339. x. [PubMed: 16198943]
52. Makris N, Meyer JW, Bates JF, Yeterian EH, Kennedy DN, Caviness VS. MRI-based topographic parcellation of human cerebral white matter and nuclei II. Rationale and applications with systematics of cerebral connectivity. Neuroimage. 1999; 9:18–45. [PubMed: 9918726]
53. Mashour GA, Walker EE, Martuza RL. Psychosurgery: past, present, and future. Brain Res Brain Res Rev. 2005; 48:409–419. [PubMed: 15914249]
54. May PR. Treatment of schizophrenia. 3. A survey of the literature on prefrontal leucotomy. Compr Psychiatry. 1974; 15:375–388. [PubMed: 4607316]
55. McGuire PK, Bench CJ, Frith CD, Marks IM, Frackowiak RS, Dolan RJ. Functional anatomy of obsessive-compulsive phenomena. Br J Psychiatry. 1994; 164:459–468. [PubMed: 8038933]
56. Meyer JW, Makris N, Bates JF, Caviness VS, Kennedy DN. MRI-Based topographic parcellation of human cerebral white matter. Neuroimage. 1999; 9:1–17. [PubMed: 9918725]
57. Moniz E. Prefrontal leucotomy in the treatment of mental disorders. Am J Psychiatry. 1937; 93:1379–1385.
58. Montoya A, Weiss AP, Price BH, Cassem EH, Dougherty DD, Nierenberg AA, et al. Magnetic resonance imaging-guided stereotactic limbic leukotomy for treatment of intractable psychiatric disease. Neurosurgery. 2002; 50:1043–1052. [PubMed: 11950407]
59. Naeser MA, Levine HL, Benson DF, Stuss DT, Weir WS. Frontal leukotomy size and hemispheric asymmetries on computerized tomographic scans of schizophrenics with variable recovery. Northampton Veterans Administration study. Arch Neurol. 1981; 38:30–37. [PubMed: 7458721]
60. Oh JS, Jang JH, Jung WH, Kang DH, Choi JS, Choi CH, et al. Reduced fronto-callosal fiber integrity in unmedicated OCD patients: a diffusion tractography study. Hum Brain Mapp. 2012; 33:2441–2452. [PubMed: 21922600]
61. Pakkenberg B. What happens in the leucotomised brain? A postmortem morphological study of brains from schizophrenic patients. J Neurol Neurosurg Psychiatry. 1989; 52:156–161. [PubMed: 2703834]
62. Pallanti S, Quercioli L. Treatment-refractory obsessive-compulsive disorder: methodological issues, operational definitions and therapeutic lines. Prog Neuropsychopharmacol Biol Psychiatry. 2006; 30:400–412. [PubMed: 16503369]
63. Perani D, Colombo C, Bressi S, Bonfanti A, Grassi F, Scarone S, et al. [18F]FDG PET study in obsessive-compulsive disorder. A clinical/metabolic correlation study after treatment. Br J Psychiatry. 1995; 166:244–250. [PubMed: 7728370]
64. Petrides M, Pandya DN. Efferent association pathways from the rostral prefrontal cortex in the macaque monkey. J Neurosci. 2007; 27:11573–11586. [PubMed: 17959800]
65. Phan KL, Fitzgerald DA, Nathan PJ, Moore GJ, Uhde TW, Tancer ME. Neural substrates for voluntary suppression of negative affect: a functional magnetic resonance imaging study. Biol Psychiatry. 2005; 57:210–219. [PubMed: 15691521]
66. Phan KL, Taylor SF, Welsh RC, Decker LR, Noll DC, Nichols TE, et al. Activation of the medial prefrontal cortex and extended amygdala by individual ratings of emotional arousal: a fMRI study. Biol Psychiatry. 2003; 53:211–215. [PubMed: 12559653]
67. Poellinger A, Thomas R, Lio P, Lee A, Makris N, Rosen BR, et al. Activation and habituation in olfaction—an fMRI study. Neuroimage. 2001; 13:547–560. [PubMed: 11305885]
68. Price JL, Drevets WC. Neurocircuitry of mood disorders. Neuropsychopharmacology. 2010; 35:192–216. [PubMed: 19693001]
69. Rademacher J, Galaburda AM, Kennedy DN, Filipek PA, Caviness VS Jr. Human cerebral cortex: localization, parcellation, and morphometry with magnetic resonance imaging. J Cogn Neurosci. 1992; 4:352–374. [PubMed: 23968129]
70. Rauch SL, Jenike MA, Alpert NM, Baer L, Breiter HC, Savage CR, et al. Regional cerebral blood flow measured during symptom provocation in obsessive-compulsive disorder using oxygen 15-labeled carbon dioxide and positron emission tomography. Arch Gen Psychiatry. 1994; 51:62–70. [PubMed: 8279930]
71. Rauch SL, Kim H, Makris N, Cosgrove GR, Cassem EH, Savage CR, et al. Volume reduction in the caudate nucleus following stereotactic placement of lesions in the anterior cingulate cortex in

humans: a morphometric magnetic resonance imaging study. J Neurosurg. 2000; 93:1019–1025. [PubMed: 11117844]

72. Rauch SL, Makris N, Cosgrove GR, Kim H, Cassem EH, Price BH, et al. A magnetic resonance imaging study of regional cortical volumes following stereotactic anterior cingulotomy. CNS Spectr. 2001; 6:214–222. [PubMed: 16951656]
73. Raz M. The painless brain: lobotomy, psychiatry, and the treatment of chronic pain and terminal illness. Perspect Biol Med. 2009; 52:555–565. [PubMed: 19855124]
74. Richter EO, Davis KD, Hamani C, Hutchison WD, Dostrovsky JO, Lozano AM. Cingulotomy for psychiatric disease: microelectrode guidance, a callosal reference system for documenting lesion location, and clinical results. Neurosurgery. 2004; 54:622–630. [PubMed: 15028136]
75. Rorden C, Karnath HO, Bonilha L. Improving lesion-symptom mapping. J Cogn Neurosci. 2007; 19:1081–1088. [PubMed: 17583985]
76. Rotge JY, Guehl D, Dilharreguy B, Cuny E, Tignol J, Bioulac B, et al. Provocation of obsessive-compulsive symptoms: a quantitative voxel-based meta-analysis of functional neuroimaging studies. J Psychiatry Neurosci. 2008; 33:405–412. [PubMed: 18787662]
77. Rotge JY, Guehl D, Dilharreguy B, Tignol J, Bioulac B, Allard M, et al. Meta-analysis of brain volume changes in obsessive-compulsive disorder. Biol Psychiatry. 2009; 65:75–83. [PubMed: 18718575]
78. Rotge JY, Langbour N, Guehl D, Bioulac B, Jaafari N, Allard M, et al. Gray matter alterations in obsessive-compulsive disorder: an anatomic likelihood estimation meta-analysis. Neuropsychopharmacology. 2010; 35:686–691. [PubMed: 19890260]
79. Schoene-Bake JC, Parpaley Y, Weber B, Panksepp J, Hurwitz TA, Coenen VA. Tractographic analysis of historical lesion surgery for depression. Neuropsychopharmacology. 2010; 35:2553–2563. [PubMed: 20736994]
80. Schwartz JM, Stoessel PW, Baxter LR Jr, Martin KM, Phelps ME. Systematic changes in cerebral glucose metabolic rate after successful behavior modification treatment of obsessive-compulsive disorder. Arch Gen Psychiatry. 1996; 53:109–113. [PubMed: 8629886]
81. Spiegel EA, Wycis HT, Marks MM, Lee AJ. Stereotaxic apparatus for operations on the human brain. Science. 1947; 106:349–350. [PubMed: 17777432]
82. Steele JD, Christmas D, Eljamel MS, Matthews K. Anterior cingulotomy for major depression: clinical outcome and relationship to lesion characteristics. Biol Psychiatry. 2008; 63:670–677. [PubMed: 17916331]
83. Stuss DTD, Benson DFD, Kaplan EFE, Weir WSW, Naeser MAM, Lieberman II, et al. The involvement of orbitofrontal cerebrum in cognitive tasks. Neuropsychologia. 1983; 21:235–248. [PubMed: 6877577]
84. Swedo SE, Pietrini P, Leonard HL, Schapiro MB, Rettew DC, Goldberger EL, et al. Cerebral glucose metabolism in childhood-onset obsessive-compulsive disorder. Revisualization during pharmacotherapy. Arch Gen Psychiatry. 1992; 49:690–694. [PubMed: 1514873]
85. Szeszko PR, Robinson D, Alvir JM, Bilder RM, Lencz T, Ashtari M, et al. Orbital frontal and amygdala volume reductions in obsessive-compulsive disorder. Arch Gen Psychiatry. 1999; 56:913–919. [PubMed: 10530633]
86. Talairach, J.; Tournoux, P. Co-Planar Stereotaxic Atlas of the Human Brain. 3-Dimensional Proportional System: An Approach to Cerebral Imaging. Thieme Medical Publishers; New York: 1988.
87. Tsuchida A, Doll BB, Fellows LK. Beyond reversal: a critical role for human orbitofrontal cortex in flexible learning from probabilistic feedback. J Neurosci. 2010; 30:16868–16875. [PubMed: 21159958]
88. Uchino A, Kato A, Yuzuriha T, Takashima Y, Kudo S. Cranial MR imaging of sequelae of prefrontal lobotomy. AJNR Am J Neuroradiol. 2001; 22:301–304. [PubMed: 11156773]
89. Waraczynski M, Zwifelhofer W, Kuehn L. Brain stimulation reward is altered by affecting dopamine-glutamate interactions in the central extended amygdala. Neuroscience. 2012; 224:1–14. [PubMed: 22906479]

90. Zald DH, Mattson DL, Pardo JV. Brain activity in ventromedial prefrontal cortex correlates with individual differences in negative affect. Proc Natl Acad Sci U S A. 2002; 99:2450–2454. [PubMed: 11842195]

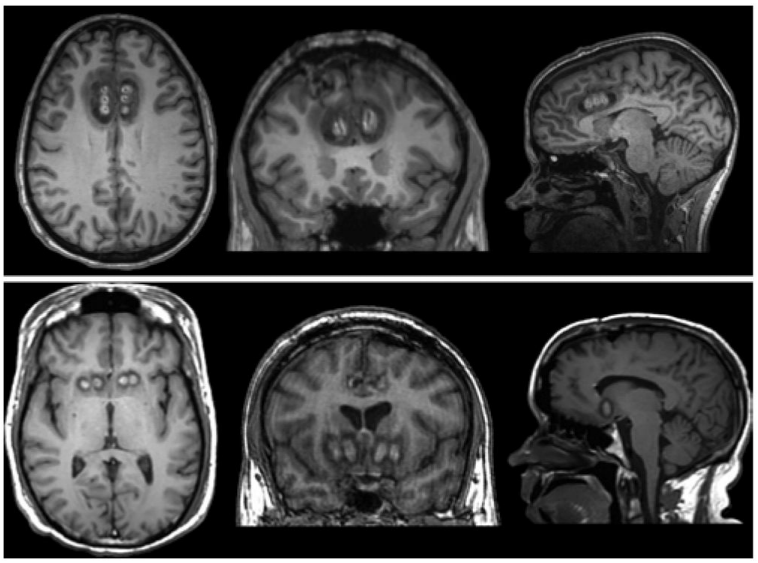

**Figure 1.**

Representative postoperative MR images of anterior cingulotomy and limbic leucotomy. **Upper:** Anterior cingulotomy. T1-weighted, magnetization-prepared rapid acquisition gradient echo axial, coronal, and sagittal images (*left* to *right*). **Lower:** Limbic leucotomy. T1-weighted axial, spoiled gradient–recalled acquisition coronal, and T1-weighted sagittal images (*left* to *right*).

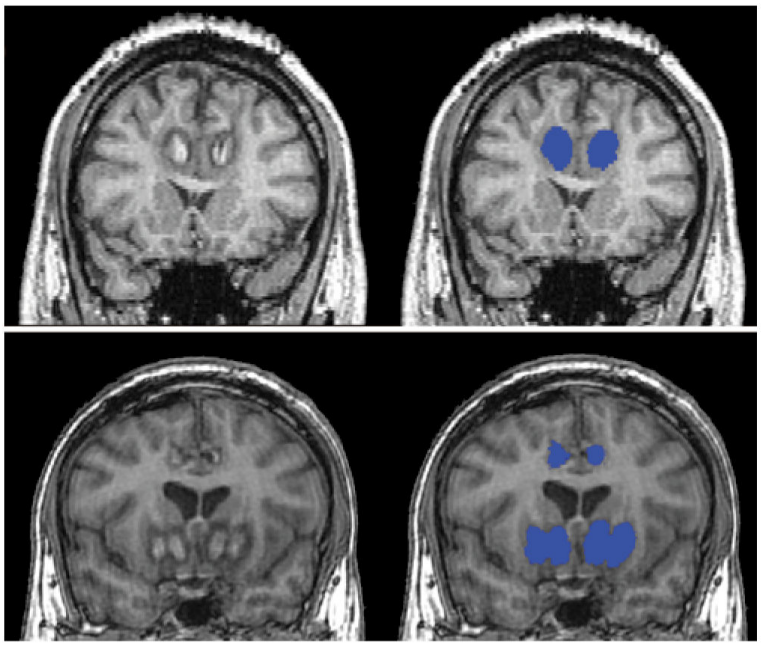

**Figure 2.**

Representative lesion masking. Lesion masks (*right*, *blue*) are shown on coronal T1-weighted MR images (*left*). **Upper:** Anterior cingulotomy. Magnetization-prepared rapid acquisition gradient echo images. **Lower:** Limbic leucotomy. Spoiled gradient–recalled acquisition images.

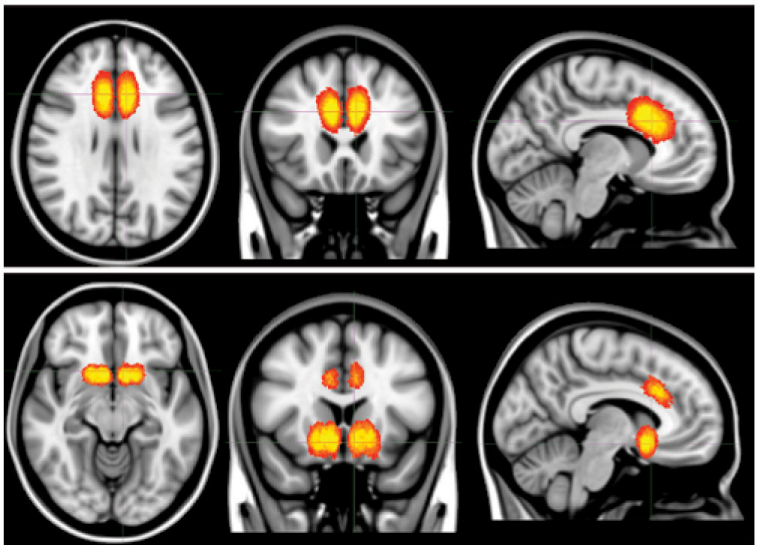

**Figure 3.**

Heat map of coregistered anterior cingulotomy and limbic leucotomy lesions. Heat maps are superimposed on the T1-weighted MNI152 template. *Yellow* indicates more lesion congruence and *red* indicates less lesion congruence. **Upper:** Anterior cingulotomy projected on axial, coronal, and sagittal T1-weighted MNI152 templates (*left* to *right*). **Lower:** Limbic leucotomy projected on axial, coronal, and sagittal T1-weighted MNI152 templates (*left* to *right*).

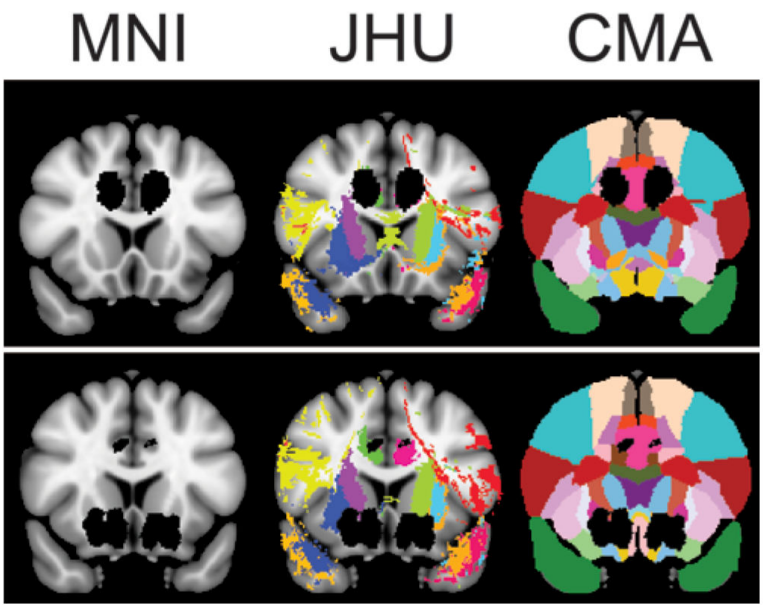


**Figure 4.**

Representative lesion mask projected on coronal T1-weighted Montreal Neurological Institute (MNI) MNI152 template, Johns Hopkins University (JHU) white-matter tractography atlas, and Center for Morphometric Analysis (CMA) structural atlas. Lesion masks are shown in black, and each color represents a unique atlas region of interest. **Upper:** Anterior cingulotomy. **Lower:** Limbic leucotomy.

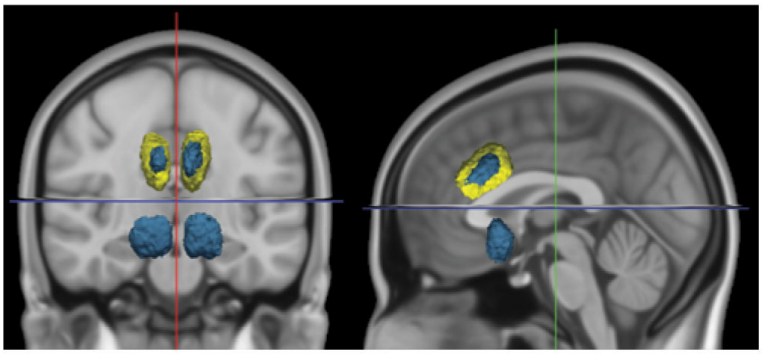

**Figure 5.**

Lesion volumetry. Three-dimensional projection of representative anterior cingulotomy *(yellow)* and limbic leucotomy *(blue)*, displayed on coronal and sagittal T1-weighted MNI152 templates (*left* to *right*).

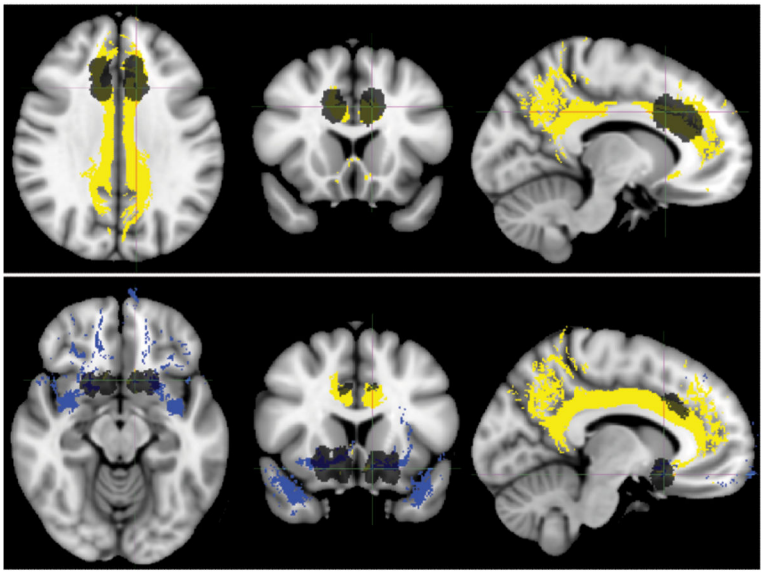

**Figure 6.**

Representative lesion masks with selected Johns Hopkins University white-matter tractography atlas ROIs. Lesions are shown in *black*. Selected ROIs are the cingulum *(yellow)* and uncinate fasciculus *(blue)*. Lesions and ROIs are projected on the T1-weighted MNI152 template. **Upper:** Anterior cingulotomy. Axial, coronal, and sagittal images (*left* to *right*). **Lower:** Limbic leucotomy. Axial, coronal, and sagittal images (*left* to *right*).

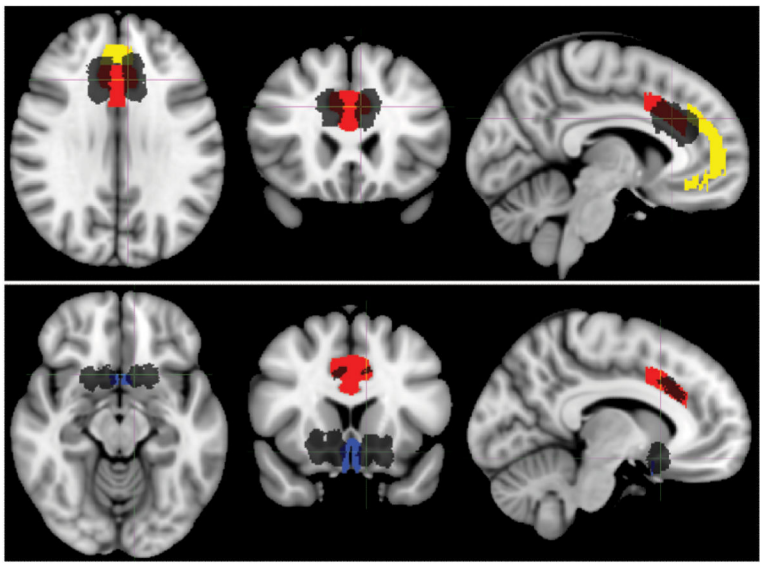

**Figure 7.**

Representative lesion masks with selected Center for Morphometric Analysis structural atlas ROIs. Lesions are shown in *black*. Selected ROIs are anteromedial cingulate gyrus, Brodmann area 24 *(red)*; paracingulate cortex, Brodmann area 32 *(yellow)*; paraterminal gyrus, Brodmann area 25 *(blue)*. Lesions and ROIs are displayed on the T1-weighted MNI152 template. **Upper:** Anterior cingulotomy. Axial, coronal, and sagittal images (*left* to *right*). **Lower:** Limbic leucotomy. Axial, coronal, and sagittal images (*left* to *right*).

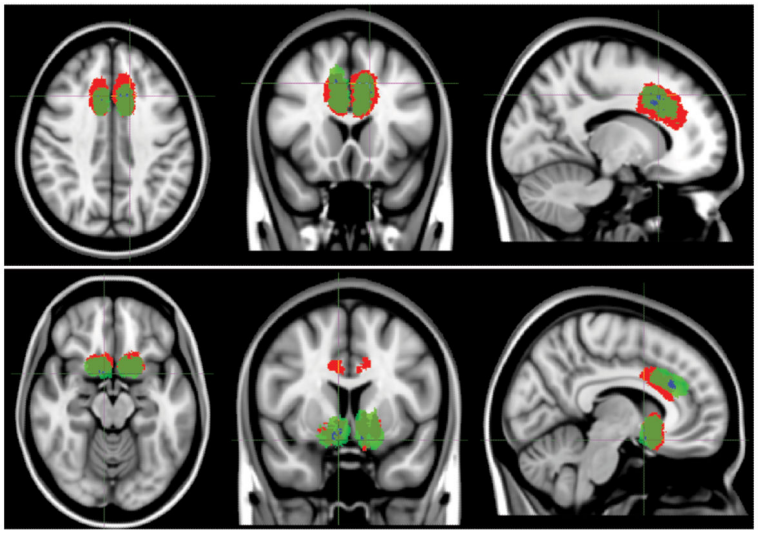

**Figure 8.**

Voxel-based lesion-outcome mapping for anterior cingulotomy and limbic leucotomy. Voxels found to be significant by VLSM are shown in *blue* (subareas within *green* areas). Nonresponder *(red)* and responder *(green)* lesion masks were collectively summed and are projected on the T1-weighted MNI152 template. **Upper:** Anterior cingulotomy. Axial, coronal, and sagittal images (*left* to *right*). **Lower:** Limbic leucotomy. Axial, coronal, and sagittal images (*left* to *right*).

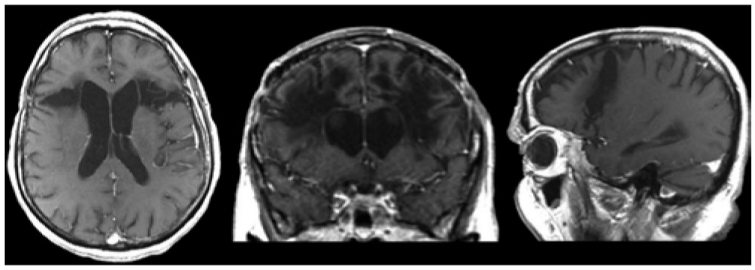

**Figure 9.**
Representative lobotomy images. Axial, coronal, and sagittal T1-weighted postcontrast MR images (*left* to *right*).

## TABLE 1

Selected anatomical overlap data for anterior cingulotomy and limbic leucotomy*

| Structure | Atlas | Mean ACT | Mean LL |
|---|---|---|---|
| lt uncinate fasciculus | JHU | | + |
| rt uncinate fasiculus | JHU | | + |
| rt cingulum | JHU | + + | + |
| lt cingulum | JHU | + + | |
| rt anteromedial cingulate gyrus, BA24 | CMA | + + + | + + |
| lt anteromedial cingulate gyrus, BA24 | CMA | + + + | + + |
| rt paracingulate cortex, BA32 | CMA | + + | |
| lt paracingulate cortex, BA32 | CMA | + + | + |
| rt paraterminal gyrus, BA25 | CMA | | + + + + |
| lt paraterminal gyrus, BA25 | CMA | | + + + |
| rt accumbens area | CMA | | + + + + |
| lt accumbens area | CMA | | + + + + |
| rt medial OFC | CMA | | + |
| rt medial OFC, white matter | CMA | | + |
| lt medial OFC | CMA | | + |
| lt medial OFC, white matter | CMA | | + + |

* Structures are shaded according to superstructure: dark gray shading = cingula and cingulate gyrus; light gray shading = orbitofrontal cortex. ACT = anterior cingulotomy; BA = Brodmann area; CMA = Center for Morphometric Analysis structural atlas; JHU = Johns Hopkins University white-matter tractography atlas; LL = limbic leucotomy; OFC = orbitofrontal cortex; + = 5%–10% overlap; + + = >10%–25% overlap, + + + = >25%–50% overlap; + + + + = >50%–100% overlap.

## TABLE 2

Follow-up data for OCD patients

| Variable | Anterior Cingulotomy | | Limbic Leucotomy | |
|---|---|---|---|---|
| | Nonresponder (n = 9)* | Responder (n = 2) | Nonresponder (n = 4)* | Responder (n = 4)* |
| mean preop Y-BOCS score | 34 ± 1.4 | 33 | 32.5 ± 2.5 | 34.8 ± 2.1 |
| most recent mean postop Y-BOCS score | 32 ± 1.5 | 11 | 27.8 ± 1.9 | 13.0 ± 4.3 |
| change in Y-BOCS score | −4.5% ± 3.3% | −66% | −13.5% ± 6.8% | −61.8% ± 12.9% |
| mean follow-up interval (mos) | 35.4 ± 13.2 | 25 | 49.0 ± 17.6 | 25.7 ± 14.5 |
| mean lesion volume (ml) | 12.8 ± 13.2 | 12.6 | 10.9 ± 1.8 | 10.5 ± 0.6 |

*Values presented as the mean ± SE.

## TABLE 3

Anatomical overlap of selected structures for anterior cingulotomy nonresponders versus responders

| | | Mean Overlap for ACT (%) | | |
|---|---|---|---|---|
| **Structure** | **Atlas** | **Nonresponders** | **Responders** | **p Value*** |
| rt cingulum | JHU | 17 | 15 | 0.6 |
| lt cingulum | JHU | 14 | 13 | 0.9 |
| rt anteromedial cingulate gyrus, BA24 | CMA | 48 | 57 | 0.4 |
| lt anteromedial cingulate gyrus, BA24 | CMA | 42 | 49 | 0.9 |
| rt paracingulate cortex, BA32 | CMA | 11 | 26 | 0.1 |
| lt paracingulate cortex, BA32 | CMA | 18 | 16 | 0.9 |

* Calculated by using the Wilcoxon rank-sum test.

## TABLE 4

Anatomic overlap of selected structures for limbic leucotomy nonresponders versus responders*

| | | Mean Overlap for Limbic Leucotomy (%) | | |
|---|---|---|---|---|
| **Structure** | **Atlas** | **Nonresponders** | **Responders** | **p Value*** |
| rt accumbens area | CMA | 69 | 87 | 0.06 |
| lt accumbens area | CMA | 76 | 87 | 0.2 |
| rt anteromedial cingulate gyrus, BA24 | CMA | 16 | 17 | 0.5 |
| lt anteromedial cingulate gyrus, BA24 | CMA | 25 | 14 | 0.1 |
| rt uncinate fasciculus | JHU | 7 | 7 | 0.7 |
| rt paraterminal gyrus, BA25 | CMA | 58 | 49 | 0.9 |
| lt paraterminal gyrus, BA25 | CMA | 25 | 31 | 0.3 |
| rt medial OFC, white matter | CMA | 10 | 5 | 0.7 |
| rt sublenticular extended amygdala | CMA | 5 | 18 | **0.03** |
| lt sublenticular extended amygdala | CMA | 9 | 15 | 0.3 |

*Calculated by using the Wilcoxon rank-sum test. Value in boldface is statistically significant.